





Original Article



Stress analysis of full-length grouted bolt under shear deformation of anchor interface

ZHU Zheng-de¹  <https://orcid.org/0000-0002-2160-8096>; e-mail: zzdj@hhu.edu.cn

SHU Xiao-yun^{1,2}  <https://orcid.org/0000-0002-0229-0350>; e-mail: shuxiaoyun211@163.com

LI Zhe⁴  <https://orcid.org/0000-0003-1974-5697>; e-mail: 775154602@qq.com

TIAN Hong-ming²  <https://orcid.org/0000-0002-4959-4212>; e-mail: hmtian@whrsm.ac.cn

TIAN Yun^{3*}  <https://orcid.org/0000-0003-4929-0347>;  e-mail: tianyun_2016@163.com

* Corresponding author

¹ College of Civil and Transportation Engineering, Hohai University, Nanjing 210024, China

² State Key Laboratory of Geomechanics and Geotechnical Engineering, Institute of Rock and Soil Mechanics, Chinese Academy of Sciences, Wuhan 430071, China

³ School of Civil Engineering, Shaoxing University, Shaoxing 312000, China

⁴ China Railway Design Corporation, Tianjin 300251, China

Citation: Zhu ZD, Shu XY, Li Z, et al. (2022) Stress analysis of full-length grouted bolt under shear deformation of the anchor interface. Journal of Mountain Science 19(11). <https://doi.org/10.1007/s11629-022-7566-4>

© Science Press, Institute of Mountain Hazards and Environment, CAS and Springer-Verlag GmbH Germany, part of Springer Nature 2022

Abstract: The bolt anchoring force is closely related to the shear properties of the anchor interface. The shear stress distribution of full-length grouted bolts is analyzed based on the stress-strain relationship among the bolt, grout, rock mass and bond interface, considering the shear properties of the grout and contact interface bonding behavior. In this case, the interfacial shear stress of the grout and rock mass and the bolt axial force are obtained under pull-out and normal working conditions. The results show that the peak shear stress of the interface with the shear deformation of the bond interface is significantly lower than that without it when the pull-out force is applied. When designing bolt parameters of grade IV and V rock mass, the relative deformation between the rock mass and anchor should be considered, with a “unimodal” to “bimodal” shear stress distribution. In the case of a low elastic modulus of rock masses, both the shear stress concentration and distribution

range are obvious, and the neutral point is near the bolt head. As the elastic modulus increases, the shear stress concentration and distribution range are reduced, and the neutral point moves towards the distal end. As a result, the optimum length of full-length grouted bolts can be determined by in-situ pull-out tests and decreases with the increased elastic modulus of the rock mass.

Keywords: Full length grouted bolt; Neutral point; Interfacial shear stress; Bolt pull out condition; Normal working condition

Notation:

Variables	Explanatory
(x, y, z)	Cartesian coordinate
$\tau, \tau_{\max}, \tau_r$	The shear stress, maximum shear stress, and residual shear stress at the contact interface
τ_1, τ_2	The shear stress of the first and second interface
δ, δ_m	The shear strain and maximum shear strain at the contact interface

Received: 18-Jun-2022

Revised: 28-Jul-2022

Accepted: 16-Sep-2022

$\delta_1, \delta_2, \gamma$	The shear strain of the first and second interface and grout
K_1, K_2, G_b	The shear modulus of the first and second interface and grout
D_1, D_2	The diameter of the bolt and borehole
G_r, E_r, μ_r	The shear modulus, elastic modulus and Poisson's ratio of rock mass
E_a	The elastic modulus of bolts
F, F_r, σ	The drawing force, additional force and stress of bolts
u_r	The displacement of the rock mass
$\varepsilon_a, \varepsilon_r$	The strain of the bolt and rock mass
$\varepsilon_{r1}, \varepsilon_{r2}$	The rock mass strain generated by drawing force and the actual working condition [Eqs. (8), (27)]
L	The length of bolts
P	The in-situ stress
β	The lining influence coefficient [Eq. (26)]
r, r_0	The radius of the rock mass and tunnel
A, B, C_1, C_2, t	The coefficient related to the rock mass characteristic and boundary [Eqs. (13), (14), (17), (25), (34)]

1 Introduction

Bolt support technology has achieved remarkable progress in the safety control of underground engineering, slope engineering in mining, water conservancy, and transportation industries. Bolt support consists of the rock mass, grout, bolt, the contact interface between the bolt and grout (the first interface) and the contact interface between the grout and rock mass (the second interface). The stress transfer behavior between the two interfaces of the three materials is the key to investigating the stress characteristics of bolts. The mechanical characteristics of full-length grouted bolts are summarized below.

You (2000, 2005) obtained the distribution of interfacial shear stress and axial force of bolts through the Kelvin displacement method and analyzed the application conditions of dispersed tension bolts. On this basis, Cao and Jiang (2003) discussed the influence of anchoring length and proposed support suggestions for different lithological conditions. However, without the shear characteristics of the anchorage contact interface, the solution of anchorage stress can only be obtained by assuming that the properties of the grout and rock mass are similar, which cannot explain the stress relationship between the different interfaces of the anchoring system. Therefore, it is necessary to analyze the coordinated

deformation relationship among bolt, grout and rock mass. Zhao (2012), He and Tian (2006), He and Zhang (2004) obtained the stress distribution of the bolt based on the coordinated deformation relationship between the grout and bolt. However, the shear properties of the interface between the rock mass and grout were also ignored, which failed to reflect the influence of the mechanical characteristics of the second interface. By comprehensively analyzing the stress-strain relationship between the bolt and grout, Farmer (1975) obtained the distribution law of shear stress for different grout thicknesses and proposed a formula of pulling resistance based on indoor pull-out tests. Delhomme and Debick (2009) added the time variable in calculating bolt drawing to verify the significant creep behavior between the bolt and rock mass in the numerical simulation and laboratory experiments. However, the analysis process cannot reflect the relationship between the anchoring mechanism and the bonding interface. In addition, some scholars used mathematical models to fit the experimental curve (Zhang and Tang 2002; Jiang 2001), which is highly accurate with simple parameters but not clear in the physical meaning and needs further study.

The pull-out test is generally a simple and inexpensive way to evaluate the in-situ load transfer efficiency of a particular support element, including laboratory and in-situ pull-out tests. According to a new laboratory test facility that enables rock bolt testing under static load conditions, Korzeniowski and Skrzypkowski (2015) found that only about 3.5% of the total deformation of all rock bolt components and displacement was attributable to the deformation of the rock bolt bar itself. Then, by developing deformable components at the rock bolt, Korzeniowski and Skrzypkowski (2017) observed two displacement phases during the static tension of the rock bolt, which differed in intensity. Based on the short bolt pull-out test, Yi et al. (2013) and Tao et al. (2022) concluded that the shear stress at the anchorage interface is not uniformly distributed even in a very short bolt, and the rock mass strength plays a significant role in increasing the pull-out load. Li et al. (2020) combined the cohesive zone model and the finite element method to prove that cohesive elements can simulate the bolt contact interface. Based on fiber Bragg grating monitoring, Duan and Mou (2020) conducted pull-out tests on 1.8 m anchors with different tensile strengths. Although the laboratory

pull-out test can reflect the stress distribution of the bolt in some ways, it is still necessary to carry out the in-situ pull-out test for the bolt because of the great differences between the field surrounding rock and the similar rock materials (e.g., concrete and epoxy resin). Richard et al. (2019) performed in-situ pull-out tests on full-length grouted bolts in clay stones. They identified one or more neutral points on most bolts. The axial strains increased from the head to the distal end of bolts during the pull-out tests. Zhao et al. (2021) analyzed the working load and ultimate load of the existing bolts by the in-situ pull-out test. They found that the peak axial force of the tested bolts was distributed at the bolt head, and the effective anchorage length of the supported rock bolt was 3 m. By a new laboratory short encapsulation pull-out test, Chen and Hagan (2016) conducted a parametric study on the axial performance of a fully grouted cable bolt. Forbes et al. (2020) performed in-situ pull-out tests with a fiber optic sensor and discussed the bolt stress and interfacial shear stress, showing that a continuous strain profile can be measured along the length of the support element under the load of the pull-out test. In conclusion, many model tests show the stress distribution of bolt by monitoring bolt axial strain, but the concepts of “the first interface” and “the second interfaces” have always been used confusedly in most case, hindering the further development of anchorage stress.

However, there is a large difference in bolt stress between the normal working condition and the pull-out test, mainly because the pull-out test cannot reflect the influence of the relative deformation between the rock mass and bolt. Freeman (1978), Wang and He (1983) proposed the neutral point theory, which divided the bolt length into anchor length and pick-up length under normal working conditions. The anchor length will decrease due to the rheological properties of the rock mass. With the development of anchorage research, the neutral point theory becomes reasonable in reflecting the actual stress condition of the bolt. Based on the deformation theory of rock mass, Li et al. (2019) analyzed the interaction of the full-length grouted bolt and the rock mass. Under normal working and near-failure conditions, the analytical formula of axial force and shear stress distribution was obtained. The results showed that the stress distribution of the interface conforms to the neutral point theory. Tao and Chen (1984), Tetsuro and Jiang (2003) provided the

formula to determine the position of the neutral point on the full-length grouted bolt. Li and Xu (2013) took the prestress as an influencing factor to analyze the coordinated deformation relationship between the bolt and rock mass. As the prestress increased, the neutral point gradually moved towards the deep rock mass, and the shear stress decreased within pick-up length but increased within anchor length. It can be seen that considering the deformation of rock mass is significant in studying the normal working condition of the bolt. If the grout and rock mass are a whole, the shear characteristics of the second interface are difficult to be reflected. Therefore, properly considering the behavior of the contact interface can help to study the mechanical characteristics of the full-length grouted bolt. Considering the plastic strength of the grout contact interface, Cai and Tetsuro (2004) proposed a method for predicting the axial force of the bolt in soft rock engineering and concluded that the debonding failure is most likely to occur near the neutral point. By the ABAQUS finite element method, Wu and Chu (2011) concluded that the deformation of rock mass increases the bolt stress and transfers the peak shear stress of the interface to the depth of the bolt. It can be seen that the shear properties of contact interfaces (the first and second interfaces) influence the anchoring mechanism. The development of the shear transfer model of the two interfaces can promote the further study of the bolt stress relationship. In the normal working conditions, bolt failure usually occurs at the contact interface between the rock mass and the grout (Wang and He 1983). When the cable bolt is grouted in a weak test material, failure always occurs along the grout-rock interface (Chen and Hagan 2016). Therefore, analyzing the shear characteristics of the second interface is crucial to investigating the force of a full-length grouted bolt.

Most studies on the full-length grouted anchorage mechanism focus on the “two materials with one interface”. The bolt and the grout are assumed to be a complex whole in studying the interface stress between the grout and rock mass. Additionally, the grout and the rock mass are assumed to be a complex whole in studying the interface stress between the bolt and the grout. Nevertheless, neither of them reflects the real mechanism of the two interfaces simultaneously. Moreover, the shear stress of the bond interface is always regarded as a function of the relative rigid

displacement on both sides of the material. However, in extensive pull-out tests of bolts (Song et al. 2018; Chai et al. 2012), a thin layer was left on the surface of bolts or drill holes, which indicates that the anchoring bond damage (Feng et al. 2022) is not a simple contact interface debonding failure, but a shear failure in the thin layer near the contact interface.

In this study, bolt stress was analyzed considering the shear displacement caused by the contact interface. Based on the stress-strain relationship among bolt, grout, rock mass, and the two interfaces (the first and second interfaces), the characteristics of the two interfaces were considered. The stress distribution of bolts was obtained under the normal working and pull-out conditions, which can provide some reference for anchor design.

2 Stress analysis of full-length grouted bolts

2.1 Anchorage physical model

Full-length grouted bolts differ significantly from end anchorages in mechanical characteristics. The force transfer behavior of the grout greatly affects the ultimate pull-out force of the bolt, and its shear stress changes the shear strain of the contact interface. Under pull-out condition, the bolt and the rock mass undergo axial deformation, and the grout undergoes shear deformation. In the interface region, the shear modulus is affected by grout properties. As the shear deformation increases, the interface unit eventually undergoes shear failure, leading to the debonding failure of the interface. In this paper, the interface between the grout, bolt, and rock mass was analyzed. The basic assumptions are as follows: (1) The rock mass, grout, and bolt are all homogeneous linear elastomers. (2) The shear stress-strain of the anchorage bond interface satisfies the linear shear model without debonding failure of the interface. (3) The influence of interfacial compressive stress on shear characteristics is not considered.

A reasonable anchorage interface shear model (including the first and second interfaces) is the key to investigating the interface mechanism of the bolt, grout and rock mass. In this paper, based on the existing test results about the shear properties of the grout, the mechanical properties of the anchorage interface are assumed, as shown in Fig 1. The shear

stress-strain relationship satisfies the following relation:

$$\tau = \begin{cases} K\delta, 0 \leq \delta \leq \delta_m \\ \tau_r, \delta > \delta_m \end{cases} \quad (1)$$

where τ represents the shear stress at the contact interface; τ_r refers to the residual shear stress at the contact interface; K is the shear modulus at the bonded contact interface; δ represents the shear strain at the contact interface; δ_m refers to the maximum shear strain at the contact interface. Since the analysis in this paper is based on the elastic assumption, the residual interface strength after peak shear stress is not considered.

2.2 Bolt stress under pull-out conditions

Under external pull-out force, the elements of bolts and grouts were analyzed, as shown in Fig. 2. According to the stress balance relationship of bolt elements in Fig. 2(a), an equation can be obtained as

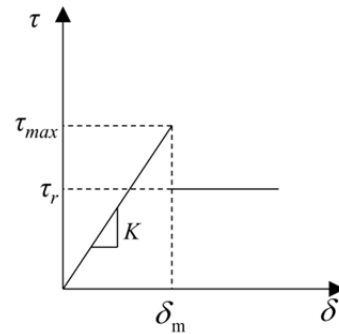


Fig. 1 Shear model of the contact interface.

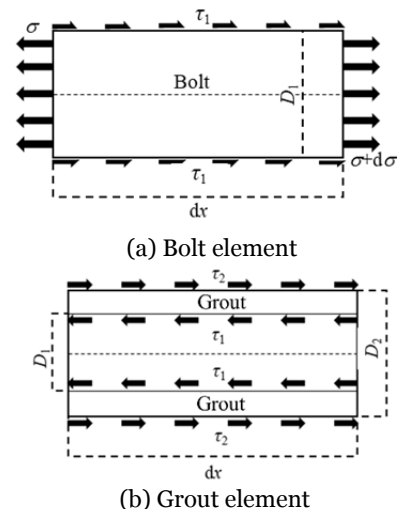


Fig. 2 Stress analysis of anchor elements.

follows:

$$\frac{d\sigma}{dx} = \frac{4\tau_1}{D_1} \tag{2}$$

where σ is the axial force of the bolt; τ_1 refers to the shear stress at the first interface; D_1 is the diameter of the bolt; x is the distance from the bolt head.

The grout transfers the external pull-out force from the bolt to the rock mass according to the shear deformation of the bolt, and the stress balance should be satisfied between the first interface and the second interface. As shown in Fig. 2 (b), an equation can be obtained as follows:

$$\tau_1 \pi D_1 dx = \tau_2 \pi D_2 dx \tag{3}$$

where D_2 is the diameter of the borehole and τ_2 is the shear stress at the second interface.

The equation can be simplified as follows:

$$\tau_1 = \frac{D_2}{D_1} \tau_2 \tag{4}$$

Since $D_2 > D_1$, τ_1 is larger than τ_2 , which is consistent with the common knowledge that the shear stress at the second interface is caused by the attenuation of the first interface. However, a simple linear attenuation was adopted in this paper. Since the shear modulus of the interface is related to the properties of the contact bodies on both sides (Song et al. 2018), an equation can be obtained as follows:

$$K = \frac{K_a K_b}{K_a + K_b} \tag{5}$$

where K is the shear modulus of the interface; K_a and K_b are the shear modulus of the two contact bodies, respectively.

Since the shear modulus of the bolt is much larger than that of the rock mass, the shear strain generated at the first interface is relatively small. Therefore, the shear stress of the second interface (hereinafter referred to as the interfacial shear stress) is important in maintaining anchorage stability (Wang and He 1983). As shown in Fig. 2(b), an equation can be obtained as follows:

$$\gamma = \frac{\tau_2}{G_b} \tag{6}$$

where γ is the shear strain of the grout; G_b is the shear modulus of the grout.

Under the pull-out condition, the coordinate deformation of the bolt, grout and rock mass should be considered. Without the influence of grout

thickness, the contact interface is regarded as a bonding element, as shown in Fig. 3. When pull-out force is applied, the shear strain of the first interface occurs due to the deformation of the bolt. According to the shear deformation of the grout, the pull-out force is transferred to the second interface and rock mass. As shown in Fig. 3, the bolt deformation includes the deformation of the rock mass, interface and grout.

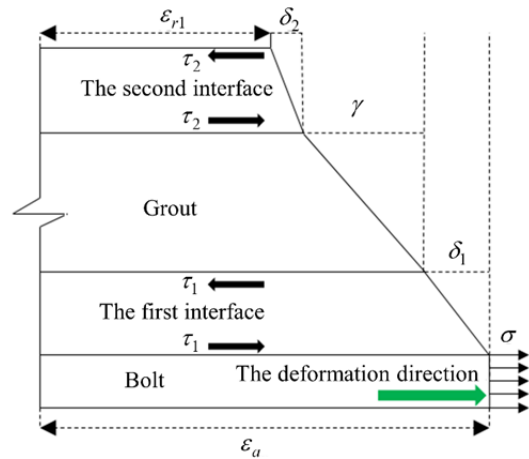


Fig. 3 Strain analysis of anchorage interface under pull-out conditions.

Compared with the scale of the rock mass, the influence of the bolt diameter can be ignored. The rock mass influenced by the bolt can be regarded as an infinite concentrated force exerted at a depth of the half-space region. As shown in Fig. 4, the vertical displacement at h can be determined by the Mindlin displacement solution. When $x=y=z=0$, the displacement of the rock mass can be expressed as:

$$u_r = \frac{(1 + \mu_r)(3 - 2\mu_r)}{2\pi E_r} \frac{F(x)}{h} \tag{7}$$

where $F(x)$ is the axial force of the bolt at position x ; E_r and μ_r are the elastic modulus and Poisson's ratio of the rock mass, respectively.

By recombining the axial direction of the bolt

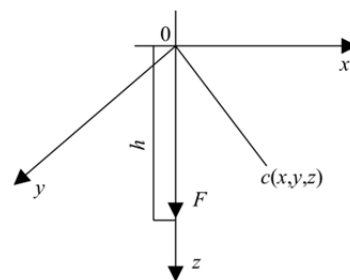


Fig. 4 Calculation diagram of Mindlin's solution.

with the z-axis and combining Eq. (3), the strain of the rock mass generated by the pull-out force can be described as:

$$\varepsilon_{r1} = \frac{du_r}{dx} = \frac{D_2(3-2\mu_r)\tau_2}{4G_r x} \quad (8)$$

where G_r is the shear modulus of the rock mass.

According to Hypothesis (2), the relationship between shear stress and shear strain at the contact interface of the grout is:

$$\begin{cases} \tau_1 = K_1 \delta_1 \\ \tau_2 = K_2 \delta_2 \end{cases} \quad (9)$$

where K_1 and K_2 are the shear modulus of the first and second interfaces; δ_1 and δ_2 are the shear strain of the first and second interfaces, respectively.

According to the physical equation of the bolt, an equation can be obtained as follows:

$$\varepsilon_a = -\frac{\sigma}{E_a} \quad (10)$$

where ε_a is the bolt strain; E_a is the bolt elastic modulus.

As shown in Fig. 3, the deformation relationship can be described as:

$$\varepsilon_a = \varepsilon_{r1} + \delta_2 + \gamma + \delta_1 \quad (11)$$

By combining Eqs. (6), (8), (9), (10) and (11), an equation can be obtained as follows:

$$(-x^2 + A)\tau_2 = (Ax + Bx^2)\tau_2' \quad (12)$$

where

$$A = \frac{D_1^2 E_a (3 - 2\mu_r)}{16G_r} \quad (13)$$

$$B = \frac{[(K_1 D_1 + K_2 D_2)G_b + K_1 K_2 (D_2 - D_1)]D_1 E_a}{4G_b K_1 K_2 D_2} \quad (14)$$

By introducing boundary conditions, we can obtain:

$$\int_0^L \tau_2 \pi D_2 dx = F \quad (15)$$

where L is the bolt length. Then, the solution of interfacial shear stress and axial force under the drawing condition can be expressed as:

$$\begin{cases} \tau_2^{(1)} = C_1 \cdot x \cdot (A + Bx)^{\frac{A}{B^2}-1} \cdot \exp\left(-\frac{x}{B}\right) \\ F_{(x)}^{(1)} = C_1 \pi D_2 \cdot (Bx + A)^{\frac{A}{B^2}} \cdot \exp\left(-\frac{x}{B}\right) \end{cases} \quad (16)$$

where C_1 is the coefficient related to the boundary, which can be described as:

$$C_1 = \frac{F}{\left[C \frac{A}{B^2} - (A + B)^{\frac{A}{B^2}} \cdot \exp\left(-\frac{L}{B}\right) \right] \pi D_2} \quad (17)$$

2.3 Bolt stress under normal working conditions

After tunnel excavation, the internal stress of the rock mass can be rebalanced to redistribute the field of stress and displacement. Especially under the soft rock condition, displacement can be significant without efficient support. Therefore, the deformation of the rock mass should be considered when designing anchorage support. The influence of rock mass deformation on bolt stress can be divided into two parts. The first part is the shear stress caused by the relative deformation between the rock mass and grout. The second one is the pull-out force applied by the anchor plate directly, which is related to the deformation of the tunnel surface. The characteristics of rock bolts are complex under the condition of soft rock filled with fracture. The bolt is subjected to not only axial tension stress but also bending failure of the transverse load. Therefore, the model presented in this paper is used to analyze one layer of the rock mass, and the anchorage of several layers of the soft rock will be researched next.

2.3.1 Relative deformation of rock mass at the interface

Due to the shear characteristics of the grout, additional shear strain is generated at the second interface when rock mass deforms toward the tunnel. The additional shear stress will be transferred to the first interface according to the shear deformation of the grout. Finally, the additional force caused by the deformation of rock mass will be balanced by the bolt deformation, as shown in Fig. 5.

For the unit additional force dF , the equation can be expressed as follows:

$$\tau_1 \pi D_1 dx = \tau_2 \pi D_2 dx = dF \quad (18)$$

In this case, the shear strain δ_2 at the second interface, the relative shear strain γ at the grout, the shear strain δ_1 at the first interface, and the bolt strain ε_a caused by the additional force can be described as:

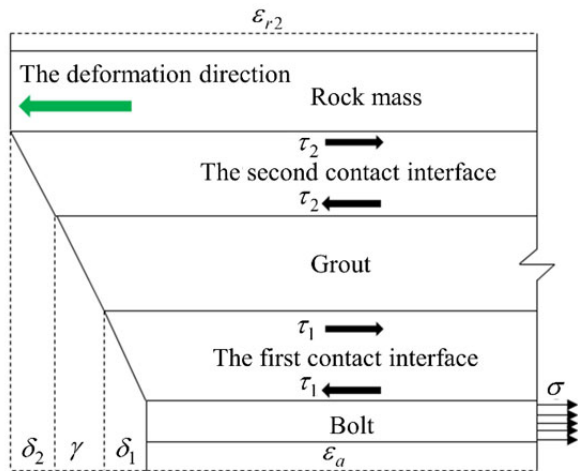


Fig. 5 Strain analysis of the anchorage interface under rock mass deformation.

$$\left\{ \begin{array}{l} \delta_2 = \frac{dF}{\pi D_2 K_2} \\ \gamma = \frac{D_2 - D_1}{G_b \pi D_1 D_2} dF \\ \delta_1 = \frac{dF}{\pi D_1 K_1} \\ \varepsilon_a = \frac{4}{\pi D_1^2 E_a} dF \end{array} \right. \quad (19)$$

Therefore, the strain of rock mass ε_Δ generated by the additional unit force dF is:

$$\varepsilon_\Delta = \delta_2 + \gamma + \delta_1 + \varepsilon_a \quad (20)$$

Assuming that $\varepsilon_{r,2}$ is the strain of rock mass caused by the bolt, the additional force of the bolt can be described as:

$$F_r = \frac{dF}{\varepsilon_\Delta} \varepsilon_{r,2} \quad (21)$$

where F_r is the additional force of the bolt. The shear stress of the second interface can be described as:

$$\tau_2 = \frac{F_r}{\pi D_2} = \frac{1}{\pi D_2} \frac{dF}{\varepsilon_\Delta} \varepsilon_{r,2} \quad (22)$$

The axial force F_r and the shear stress τ_2 satisfy the relation:

$$F_r + \int_0^r \pi D_2 \tau_2 dr = 0 \quad (23)$$

Then the differential equation of the strain of rock mass influenced by the bolt is:

$$\varepsilon_{r,2} + \varepsilon'_{r,2} = 0 \quad (24)$$

The general solution of the upper differential equation can be obtained as follows:

$$\varepsilon_{r,2} = C_2 \cdot e^{-r} \quad (25)$$

Due to the lining and other constraints at the tunnel surface, the bolt head can be coordinated under the strain condition. Namely, when r equals r_0 , the rock strain at the tunnel surface can be expressed as:

$$\varepsilon_{r,2|_{r=r_0}} = \frac{P\beta}{2G_r} \quad (26)$$

where β is the influence coefficient of lining, which can be obtained by the formula of elastic mechanics; r_0 is the radius of the tunnel; P is the in-situ stress. Therefore, the strain of rock mass under the anchorage support can be described as:

$$\varepsilon_{r,2} = \frac{P\beta}{2G_r} \cdot e^{-r+r_0} \quad (27)$$

The deformation law of rock mass under the influence of the anchor is consistent with the result of Song et al. (2018). Therefore, considering the deformation of rock mass after tunnel excavation, the distribution of interfacial shear stress $\tau_2^{(2)}$ and the axial force of bolts $F_{(x)}^{(2)}$ can be expressed as:

$$\left\{ \begin{array}{l} \tau_2^{(2)} = \frac{1}{\pi D_2} \cdot \frac{1}{\varepsilon_\Delta} \cdot \frac{P\beta}{2G_r} \cdot e^{-x} \\ F_{(x)}^{(2)} = \frac{1}{\varepsilon_\Delta} \cdot \frac{P\beta}{2G_r} \cdot e^{-x} \end{array} \right. \quad (28)$$

2.3.2 Effect of the anchor plate

According to Hypothesis (1), the action of the anchor can be considered a superposed process. The resilient stress reversely acts on the rock mass after the prestress is applied to the bolt. Thus, the displacement of the rock mass surface departing from the tunnel can be described as:

$$\Delta U_1 = \int_0^L \varepsilon_{r,1} dx \quad (29)$$

Considering the deformation of rock mass, the displacement of the tunnel surface to the tunnel can be described as:

$$\Delta U_2 = \int_{r_0}^{r_0+L} \varepsilon_{r,2} dr \quad (30)$$

After substituting into Eqs. (8) and (26), the relative displacement between the bolt and rock mass

under the influence of excavation and prestress can be described as:

$$\Delta U_3 = -\frac{D_2(3-2\mu_r)}{4G_r} \cdot C_1 \cdot \frac{B}{A} \left[\frac{(A+BL)^{A/B^2}}{A+1+BL} \cdot \exp\left(-\frac{L}{B}\right) - \frac{A^{A/B^2}}{A+1} \right] + \frac{P\beta}{2G_r} \cdot (1-e^{-L}) \quad (31)$$

Due to the restraint of the anchor plate, the relative displacement between the bolt and the rock mass is limited. In this case, the tunnel surface and the bolt head should maintain a coordinate deformation relationship, i.e., no relative slip between them. Therefore, the relative displacement of the bolt and rock mass should be converted into the additional force of the bolt ΔF , which is expressed as:

$$\Delta F = \Delta U_3 E_a \frac{\pi D_1^2}{4} \quad (32)$$

According to the research by You (2000), the distribution of the interfacial shear stress and axial force of bolts caused by additional forces can be described as:

$$\begin{cases} \tau_2^{(3)}(x) = \frac{2\Delta F}{\pi D_1} \cdot \left(\frac{tx}{2}\right) \exp\left(-\frac{t}{2}x^2\right) \\ F_{(x)}^{(3)} = \Delta F \cdot \exp\left(-\frac{t}{2}x^2\right) \end{cases} \quad (33)$$

where

$$t = \frac{4}{(1+\mu_r)(3-2\mu_r)D_1^2} \left(\frac{E_r}{E_a}\right) \quad (34)$$

Under the normal working condition, the stress of the anchorage can be divided into three parts:

1. The bolt tension departs from the tunnel due to prestress;
2. The additional stress of the interface pointing to the tunnel due to the deformation of the rock mass;
3. The additional stress of the bolt pointing to the tunnel due to the deformation of the anchor plate.

When the analyzed object exceeds prestress, the first stress can be set to zero. If only rock mass deformation is considered, the stress distribution characteristics of the bolt can be described. Assuming that the direction departing from the tunnel is the positive direction of the second interface, the interfacial shear stress and axial force of bolts under the combined influence of the three parts can be described as:

$$\begin{cases} \tau_2(x) = -C_1 \cdot x \cdot (A+Bx)^{\frac{A}{B^2}-1} \cdot \exp\left(-\frac{1}{B}x\right) - \frac{1}{\pi D_2} \cdot \frac{1}{\varepsilon_\Delta} \cdot \frac{P\beta}{2G_r} \cdot e^{-x} + \frac{2F}{\pi D_1} \cdot \left(\frac{tx}{2}\right) \exp\left(-\frac{t}{2}x^2\right) \\ F(x) = C_1 \pi D_2 \cdot (Bx+A)^{\frac{A}{B^2}} \cdot \exp\left(-\frac{x}{B}\right) + \frac{1}{\varepsilon_\Delta} \cdot \frac{P\beta}{2G_r} \cdot e^{-x} - \Delta F \cdot \exp\left(-\frac{t}{2}x^2\right) \end{cases} \quad (35)$$

3 Numerical simulation of Full-Length Grouted Bolts Considering Interface Deformation

3.1 Stress characteristics of the bolt under the pull-out condition

The pull-out test is generally simple and inexpensive to evaluate the in-situ load transfer efficiency of a particular support element (Korzeniowski and Skrzypkowski 2015, 2017). However, there are limitations regarding the ability of the pull-out test to function as a support performance characterization technique, such as the external nature of measurement techniques during testing. Therefore, numerical simulation has become an effective way to analyze the stress distribution of bolts. Li et al. (2020) combined the cohesive zone model and the finite element method to demonstrate that cohesive elements can effectively simulate the contact of the bolt interface.

According to the pull-out test of the full-length grouted bolt (Zhao et al. 2021; Korzeniowski and Skrzypkowski 2017), the diameter of the bolt is set to 22 mm, the diameter of the borehole is set to 50 mm, and the elastic modulus of the bolt is set to 210 GPa. According to the property of the existing mortar grout and the supporting conditions of the soft rock tunnel, the elastic modulus of the grout is 30 GPa, and that of the rock mass is 4 GPa. The bolt length is 4 m, and the Poisson's ratio of all materials is 0.25. The shear modulus of the bolt is greater than that of the grout and rock mass, which significantly enhances the shear stiffness of the first interface, leading to a much larger K_1 value than K_2 . According to Eq. (5) and reference (Zhu 2007), the interface parameters are set as $K_1=83.6$ GPa/m and $K_2=9.95$ GPa/m. The bolt support was tested by applying a static pull-out load in ABAQUS, as shown in Fig. 6(a). The rock mass was surrounded by a fixed boundary of 1 m×1 m×4 m in

size. The contact interface between the bolt, grout and rock mass was simulated by the cohesive element, as shown in Fig. 6(b). After the bolt, grout and rock mass were meshed, the cohesive element was inserted in the contact interface and divided the initial grid point into two groups belonging to different parts. When the relative displacement of the grid point occurred between the two groups, the shear stress was transferred under the action of shear stiffnesses K_1 and K_2 . The Q-S (load-displacement) curve obtained from the numerical simulation and in-situ pull-out test is presented in Fig. 6(c). With the increase in the bolt head displacement, the load of the bolt increases nonlinearly to a constant (about 200 kN), which is consistent with the result of the in-situ pull-out test and verifies the effectiveness of the numerical simulation test.

The stress on the bolt under the pull-out condition is caused by the overall action of the bolt, grout, rock

mass and bonding interface. The shear properties of the interface exert an important influence on the stress distribution of the bolt. Without the shear deformation of the interface, You (2000) presented a traditional analytical solution for the interfacial shear stress under the pull-out condition. To obtain the stress distribution of the bolt and interface, the pull-out force is set to 50 kN. Fig. 7 shows the comparison among numerical simulation results, the model proposed in this paper, and the solution of You (2000).

The numerical results are in good agreement with the model presented in this paper, indicating that the contact interface model based on “three materials and two interfaces” can reflect the internal mechanical behavior of the anchor. Since the traditional calculation model excludes the shear deformation of the grout, the axial force of bolts and interfacial shear stress are mainly distributed in a small range near the

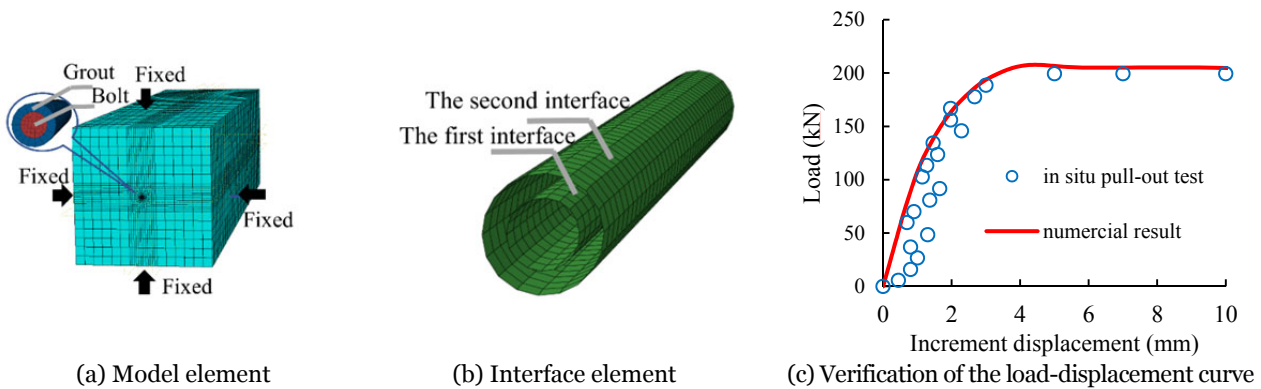


Fig. 6 Model schematic of pull-out tests.

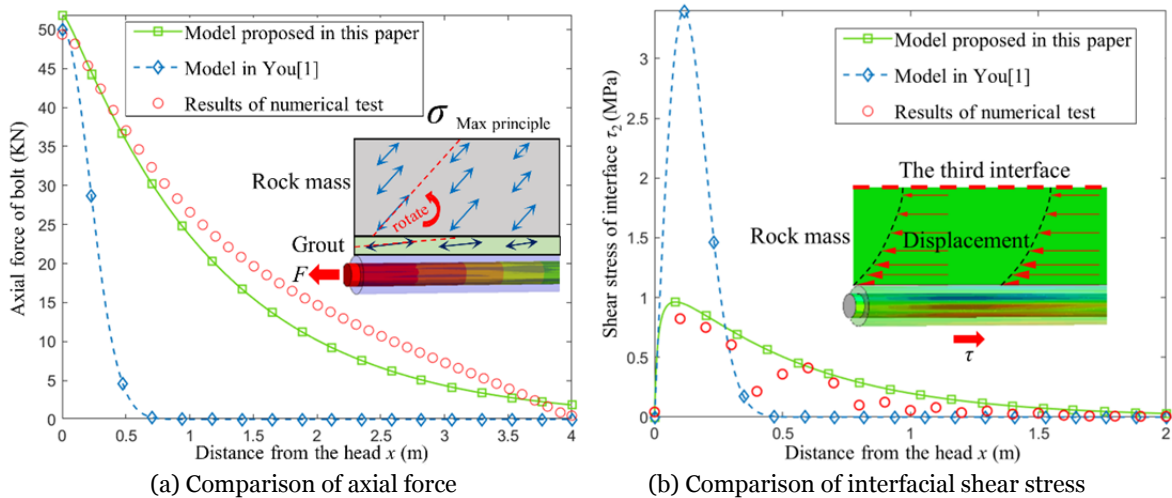


Fig. 7 Comparison between theoretical and numerical results of axial force and interfacial shear stress under the pull-out condition.

bolt head, which is similar to the phenomenon that the internal stress of the rigid body is significantly concentrated. Thus, if the shear deformation of the grout and contact interface is not considered, the degree of shear stress concentration will be significantly greater than the actual situation. When the grout is not considered a rigid body, the interfacial shear stress and the axial force of bolts will gradually transfer to the deep part under the shear deformation of the grout and contact interface. As the shear modulus of the grout increases, its peak shear stress decreases while the range of interfacial shear stress increases significantly. However, due to the limited deformation capacity of the grout, the stress concentration near the bolt head is obvious. The region near the bolt head is the most susceptible to fracture and debonding failure when the pull-out force is applied. Assuming that the deformation of the contact interface is infinite, i.e., the shear modulus of the grout is zero, the interfacial shear stress is not involved in sharing the axial force of the bolt. In this case, the bolt stress shifts to the end anchorage, and the axial stress distributes along the full bolt evenly. Because the pull-out force is borne by the bolt, its stress is easier to reach the tensile strength, which leads to the destruction.

According to the numerical simulation results, the interfacial shear stress is smaller than the numerical value obtained from numerical results, as shown in Fig. 7 (b). The reason is that the rock mass deformation near the bolt surface is not uniformly distributed but decays in an uncertain law along the direction perpendicular to the rock bolt. The rock mass shear deformation boundary caused by the action of bolts is called “the third interface”, which is not considered in this paper because its boundary is difficult to determine. As analyzed in subsection 1.2, bolt deformation consists of the deformation of the rock mass, interface and grout. Thus, the reduction of rock mass deformation will directly influence the shear stress of the interface. Due to the obvious difference between the grout and rock mass, the maximum principal stress of the two materials will be significantly deflected, as shown in Fig. 7(a). The pull-out force is transferred from the grout to rock mass under the action of shear deformation at the second interface, causing a major difference in the stress state between the grout and rock mass and significantly increased bolt load length. Therefore, it is important to consider the characteristics of the contact interface

between the bolt, grout and rock mass.

3.2 Stress characteristics of the bolt under normal working conditions

Different from the pull-out condition, the normal working condition of the bolt is affected by the deformation of the rock mass. Bolt support changes from passive to active, and the distribution of the interfacial shear stress changes greatly. By installing full-length grouted bolts in clay stones, Richard et al. (2019) monitored the distribution of bolt axial stress and found one or more neutral points on most bolts. Ignoring the influence of lining and prestress, the CT bolt 2 (no weak interface exists) was selected to verify the model proposed in this paper. The first term of Eq. (34) is set to 0, and β equals 1. Fig. 8 shows the comparison between the model proposed in this paper and the in-situ monitoring results of Richard et al. (2019).

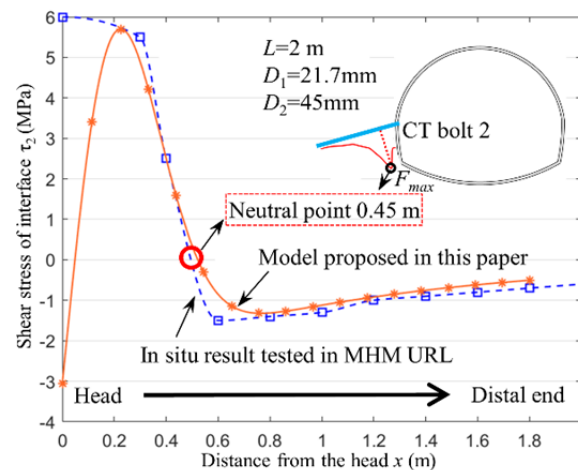


Fig. 8 Verification of interfacial shear stress under normal working conditions.

1) The model proposed in this paper is basically consistent with the in-situ monitoring results, indicating that it can reflect the stress distribution of the bolt under normal working conditions. Due to the limitation of the anchor plate, the deformation of the rock mass at the bolt head is coordinated, and the peak point of the interfacial shear stress gradually moves from the bolt head to the distal end. Thus, interfacial shear stress changes from nonlinear attenuation to unimodal distribution.

2) Under normal working conditions, the distribution characteristics of interfacial shear stress prove the existence of the neutral point in the full-

length grouted bolt, and its position is closely related to the peak position of shear stress. Due to the deformation of rock mass, a neutral point with zero shear stress exists at the contact interface. From the bolt head to the neutral point, called the “pick-up length”, the interfacial shear stress points to the tunnel to limit rock mass deformation. From the neutral point to the bottom of the bolt, the “anchor length”, the interfacial shear stress returns to the tunnel direction to limit bolt deformation. Thus, the neutral point becomes the demarcation point for the stress direction of the bond interface, where the bolt axial stress is maximum, as shown in Fig. 8. In this case, the neutral point is about 0.45 m away from the bolt head, which is consistent with the results obtained from in-situ monitoring.

3) The interfacial shear stress transforms from “unimodal” to “bimodal” distribution under normal working conditions compared with the pull-out condition, and the peak position of shear stress can be determined by in-situ pull-out tests. When the deformation of rock mass is considered, the interfacial shear stress rapidly peaks (maximum positive shear stress) near the bolt head. The peak position is consistent with that under the pull-out condition. After neutral point reversion, the interfacial shear stress attenuates rapidly to the second peak (maximum negative shear stress), but the magnitude is much smaller than the first one, implying that the shear failure caused by the interface is more likely to occur in the pick-up length. In this case, the peak position of interfacial shear stress can be found by in-situ pull-out tests when designing the bolt, and the bond strength of the pick-up length should be enhanced to maintain anchorage stability.

4 Influence of rock mass properties on bolt stress characteristics

4.1 Influence of the rock mass on bolt stress under the pull-out condition

Due to the variability of rock mass conditions, the properties of the rock mass should be fully considered when designing anchorage parameters. The shear properties of the grout are ignored in most traditional methods, which cannot reflect the bolt stress. The properties of the grout and contact interface have an important impact on bolt stress. Therefore, with different elastic moduli of the rock mass, it is

necessary to compare the mechanical characteristics of the bolt with and without considering the shear deformation of the interface.

According to Fig. 9, conclusions can be drawn as follows:

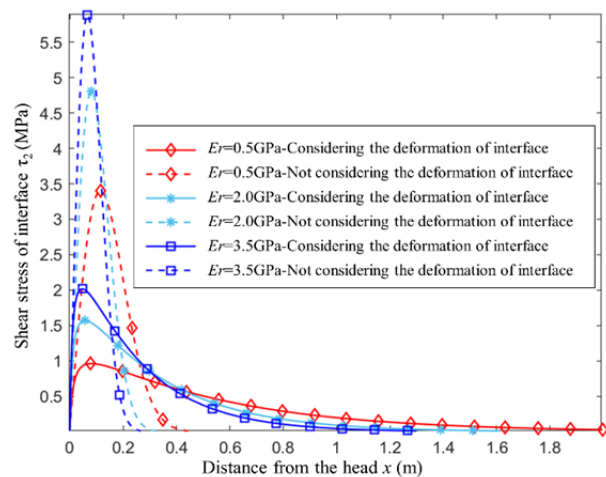


Fig. 9 Influence of lithological conditions on shear stress.

1) Under the same elastic condition, the distribution law of interfacial shear stress is basically the same regardless of the consideration of anchorage interface deformation. The shear stress presents an obvious unimodal distribution in the region of 1/3 near the bolt head and decreases rapidly after reaching the peak. As the elastic modulus of the rock mass increases, the peak values of both shear stress gradually rise, and the peak slowly moves towards the bolt head.

2) The shear deformation of the contact interface can significantly affect the distribution range of shear stress and reduce the peak shear stress. When the elastic moduli of the rock mass are 0.5 GPa, 2 GPa and 3.5 GPa, the distribution ranges of interfacial shear stress are 0.46 m, 0.33 m and 0.25 m without considering the shear deformation of the contact interface and 2.5 m, 1.8 m and 1.4 m when it is considered. The distribution range of shear stress is expanded, and the peak shear stress is significantly reduced.

3) The anchoring parameters can be designed more reasonably when considering the influence of the grout and the shear deformation of the contact interface. When the bolt is subjected to pull-out force, both the grout and the contact interface participate in the coordinated deformation process of the anchoring system. The interfacial shear stress concentration is

reduced, and its distribution is more uniform through shear deformation inside the bolt. However, if the influence of shear deformation is ignored, the concentration degree and distribution range of interfacial shear stress will be misestimated during the anchoring design. The bolt length is short, which results in excessive shear strength at the interface and insufficient bolt strength. Therefore, the bolt is easily damaged under tensile failure.

4.2 Influence on bolt stress under normal working conditions

4.2.1 Stress distribution of the interface and bolt

As one of the main factors to be considered, rock mass deformation plays an important role in designing bolts. The excavation depth and the elastic modulus of the rock mass determine the support parameters of tunnel excavation and affect the stress distribution of the anchorage interface and bolt. The elastic moduli of the rock mass are set to 0.5 GPa, 2 GPa and 3.5 GPa, and in-situ stress conditions are 5 MPa, 10 MPa and 15 MPa. The stress distributions of the interface and bolt are shown in Fig. 10 and Fig. 11, respectively.

By comparing the stress distribution law of the interface and bolt under different in-situ stresses and elastic moduli of the rock mass, it can be known that:

1) Under the normal working condition, ensuring the shear stress strength of the pick-up length and the bolt tensile strength of the neutral point is the key to controlling the anchorage stability. Under different rock mass conditions, the distribution of interfacial shear stress is basically the same. There is always a “neutral point” that divides the bolt into pick-up length and anchor length, and the first peak shear stress of the interface in the pick-up length is always greater than the second one in the anchor length. Due to the deformation of the rock mass, the anchorage force mechanism evolves from passive drawing to active support, causing a great difference between the axial force distribution of the bolt and the peak axial force of the bolt head under the pull-out condition. Because the interfacial shear stress on both sides of the neutral point is in the opposite direction, the axial force of the bolt reaches the maximum at the neutral point. Thus, the neutral point is the most vulnerable position for failure. In designing the bolt, the stability of the neutral point should be particularly checked if

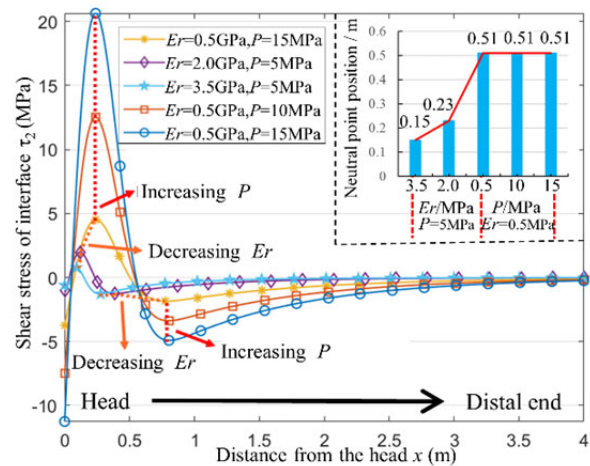


Fig. 10 Distribution of interfacial shear stress under different deformation conditions of the rock mass.

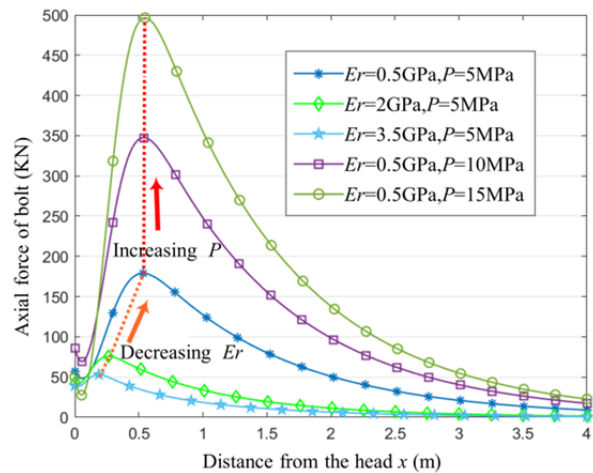


Fig. 11 Distribution of the axial force of bolts under different deformation conditions of the rock mass.

the extension strength meets the requirements.

2) The elastic modulus of the rock mass has different effects on the interfacial shear stress and the bolt axial force, and the maximum positive shear stress is affected more significantly. When the in-situ stress is 5 MPa, the peak shear stress of the interface and the bolt axial force gradually increase as the elastic modulus of the rock mass decreases. The peak shear stress gradually moves to the distal end of the bolt, while the peak axial force always stays at the neutral point. When the elastic modulus of the rock mass changes from 3.5 GPa to 2 GPa and 0.5 GPa, the maximum positive shear stress increases by 160% and 128%, while the maximum negative shear stress increases by 0.96% and 47.3%, respectively. The peak axial force increases by 41% and 136%, respectively. It can be seen that the influence of the maximum

positive shear stress is gradually weakened while the maximum negative shear stress and the bolt axial force gradually increase with the decreasing elastic modulus of the rock mass. Thus, in deep soft rock tunnels, the property of the rock mass is the key to controlling the deformation and stability behavior of tunnels.

3) The distribution law of interfacial shear stress and bolt axial force is basically consistent with that of in-situ stress. Their magnitude is significantly affected by the changes in in-situ stress. With the increase in in-situ stress, the interfacial shear stress and the axial force of the bolt increase significantly, while the change in the peak stress is not significant. When the in-situ stress increases from 5 MPa to 15 MPa, the maximum positive shear stress increases by 178% and 64.7%, while the maximum negative shear stress increases by 83.1% and 45.5%, and the axial force increases by 94.4% and 42.9%, respectively. Thus, the influence of the peak stress of the interface and bolt reduces gradually with increasing in-situ stress, indicating the necessity of anchor support during deep tunnel excavation.

4) Rock mass deformation also has a significant impact on bolt failure. When the deformation of the surrounding rock is large, the maximum positive shear stress is much larger than the maximum negative shear stress, and the shear stress of the contact interface is concentrated in the pick-up length. The interface stress condition is poor, and shear failure easily occurs. As the deformation of the surrounding rock decreases, the difference between the maximum positive shear stress and the maximum negative one reduces. The distribution of shear stress at the contact interface is gradually uniform. With the improvement of interfacial stress conditions, the shear failure of the interface is relatively difficult to occur, and the extension strength of the bolt becomes the key to controlling anchorage stability. Thus, to ensure the long-term stability of the anchorage system, both the shear strength of the interface and the extension strength of the bolt should be considered in deep soft rock engineering.

4.2.2 Neutral point and the optimal anchor length

According to the distribution law of interfacial shear stress under different rock mass conditions, the position of the neutral point almost does not change with the in-situ stress but is affected by the elastic

modulus of the rock mass. As the elastic modulus of the rock mass decreases, the neutral point gradually moves to the depth of the bolt under the influence of prestressing and deformation of the rock mass. Therefore, a higher elastic modulus of the rock mass indicates that the neutral point is closer to the bolt head, which is consistent with the result of Tetsuro (2003). The neutral point position of Tetsuro (2003) and that of the model proposed in this paper are compared in Table 1. The position of the neutral point for the bolt lengths tested is shown in Fig. 10. At the same in-situ stress, when the elastic moduli of the rock mass are 3.5 GPa, 2.0 GPa, and 0.5 GPa, the positions of the neutral point are 0.21 m, 0.35 m, and 0.51 m, respectively. As the in-situ stress increases from 5 MPa to 15 MPa, the neutral point remains essentially unchanged, indicating that the neutral point mainly relates to the characteristics of the rock mass rather than the in-situ stress. The position of the neutral point proposed in this paper is close to the result of Tetsuro (2003) when the elastic modulus of the rock mass is low. However, the depth of the neutral point is smaller than the result of Tetsuro (2003) as the elastic modulus of the rock mass increases, mainly because the model in this paper takes the grout as a separate transfer medium to establish a relationship among the rock mass, grout and bolt, while Tetsuro (2003) treats the bolt and grout as a uniform medium. When the elastic modulus of the rock mass is low, its deformation is large. The bolt and grout can be regarded as a uniform medium because grout deformation is smaller than rock mass deformation. However, as the elastic modulus of the rock mass increases, the relative deformation of the grout cannot be ignored due to the decreasing rock mass deformation. Therefore, under the influence of interfacial shear stress caused by the rock mass deformation, the neutral point moves towards the bolt head without considering the grout deformation.

Table 1 Influence of rock properties on bolt parameters ($P=5$ MPa)

Elastic modulus (GPa)	Recommended bolt length (m)	Neutral point in this paper (m)	Neutral point of Tetsuro ESAKI	Pick-up ratio* (%)
0.5	4.0	0.51	0.68	12.75
2	2.5	0.23	0.67	9.7
3.5	2.0	0.15	0.62	8

Notes: *, pick-up length to bolt length.

When the elastic modulus of the rock mass changes from 0.5 GPa to 3.5 GPa, the pick-up ratio decreases slightly with the decrease in effective anchorage length, indicating that the neutral point and the effective anchorage length change synchronously under different lithological conditions. Considering the safety stock, the pick-up ratio can be set to 20%. Therefore, in designing the bolt, the pick-up length can be estimated based on the shear stress position of the interface by the in-situ pull-out test first. Then, the optimal length of the bolt can be determined according to the pick-up ratio. Table 1 shows the recommended bolt length under different rock mass conditions, taking the in-situ stress of 5 MPa as an example. The softer rock mass means that the longer bolt should be adopted because the shear stress distribution of the interface and bolt is wide and uneven. In contrast, short bolts should be used for hard rock masses. Moreover, in soft rock engineering, the long-term stress stability of the bolt should be considered because its stress condition is too poor to keep the shear stability of the interface. In hard rock engineering, the anchor can maintain excavation stability because it has better stress conditions.

5 Discussion

The influence of rock mass deformation is a comprehensive indicator that should conform to engineering requirements. In engineering, where the deformation is strictly controlled, the lining with large stiffness is often combined with the bolt system. In this case, the influence of rock mass deformation can be negligible in the bolt support design because it is very small. However, for some large deformation projects, the yielding supporting technique is often adopted to reduce the stress of the lining structure, and the influence of rock mass deformation cannot be ignored. The stress distribution law of full-length grouted bolts varies greatly under different rock mass conditions. With the increased excavation depth of the tunnel, the in-situ stress and prestress are taken as 5 MPa and 50 KN, respectively. The influence of rock mass deformation at different lithological grades (Li 2014) is shown in Table 2. The shear stress distribution with and without rock mass deformation is shown in Fig. 12.

When designing the bolt, whether the

Table 2 Influence of different rock grades on interfacial shear stress

Grade of rock mass	Elastic modulus E_r (Gpa)	Poisson's ratio ν	Deformation of rock mass
III	15	0.25	Can be ignored
IV	3.5	0.32	Should not be neglected
V	0.5	0.36	Should not be neglected

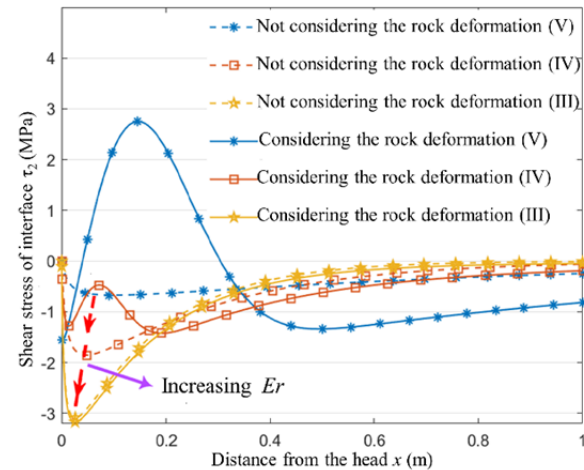


Fig. 12 Distribution of interfacial shear stress at different rock mass grades.

deformation of rock mass is considered greatly influences the analysis of the bolt. Under the condition of V rock mass, the peak shear stress with a significant influence of rock mass deformation increases by three times compared with that without the influence of rock mass deformation. The distribution form of shear stress conforms to the neutral point theory. In this case, the influence of rock mass deformation should be fully considered instead of simply adopting pull-out tests when designing bolt parameters. As the rock mass grade increases to IV, the additional interfacial shear stress and the bolt axial force from the deformation of rock mass decrease, which reduces the differences in the bolt stress with and without rock mass deformation. When the rock mass grade increases to III, the influence of rock mass deformation can be ignored because the distribution of interfacial shear stress in the two analysis modes is basically the same. With the further increase of rock mass grade, the rock mass deformation can be neglected after excavation and support because it is extremely small. Therefore, under the conditions of IV and V rock mass, the deformation of rock mass should be considered in designing anchorage parameters. When the grade of

rock mass is greater than III, the influence of rock mass deformation on the bolt stress can be ignored.

Due to the simplified mechanical properties of the interface, this analytical model may have some shortcomings and inapplicable cases. For example, in some bolts with rough surfaces, the load-displacement curve of the bolt approximates ideal elastoplastic. The model proposed in this paper needs to consider the residual strength when the friction effect of the bolt surface is obvious. Under extremely weak rock mass conditions, wedge-shaped failures may occur inside the rock mass under the pull-out force of bolts. The model proposed in this paper may be no longer suitable because the influence of “the third interface” is not considered. Particularly, under the condition of soft rock filled with fractures, filling cracks by high-pressure grouting can improve the stability of the rock mass. The shear and open effect of fracture should be considered when analyzing the bolt stress, and the transverse shear load of bolts is dominant rather than the axial load. Additionally, the diameter of the borehole should be replaced with the range of grouting reinforcement.

6 Conclusions

The properties of the contact interface, including the bolt-grout interface (the first interface) and the grout-rock mass interface (the second interface), have an important influence on the analysis of bolt stress. Based on elastic shear stress-strain theory, the distribution of interfacial shear stress and axial bolt stress are obtained under pull-out and normal working conditions considering the shear deformation of the interface, which provides a theoretical basis for the design of the full-length grouted bolt.

Under the pull-out condition, the peak shear stress of the interface decreases and the distribution range increases under the influence of shear deformation of the interface and grout, which can better describe the behavior of bolt stress under the pull-out force. As the elastic modulus of the rock mass increases, the peak shear stress of the interface increases, and the peak moves towards the bolt head. Numerical studies show that the rock mass

deformation near the bolt surface is not uniformly distributed but decays in a nonlinear law along the direction perpendicular to the rock bolt. The direction of the maximum principal stress between the grout and rock mass differs greatly due to the shear deformation of the interface, which plays an important role in increasing the load length of bolts.

Under the normal working condition, the shear stress of the interface has a neutral point near the bolt head, and its position is closely related to that of peak shear stress. With the increased elastic modulus of the rock mass, the neutral point moves towards the bolt head. The optimum bolt length can be determined by in-situ pull-out tests because the ratio of pick-up length to bolt length varies in the range of 0.2. Compared with the “unimodal” distribution in pull-out conditions, the shear stress of the interface changes to a “bimodal” distribution under the influence of rock mass deformation. The bolt failure always starts from the pick-up length and develops to the depth of the bolt due to the maximum shear stress within the pick-up length.

The properties of the rock mass significantly influence the anchorage failure mode. Under soft rock mass conditions, the distribution range of interfacial shear stress is large, and the shear stress of the pick-up length is significantly greater than that of the anchor length. In this case, the longer bolt should be used for support because the bolt is easily pulled out due to the debonding failure of the interface. As the elastic modulus of the rock mass increases, the distribution range of interfacial shear stress decreases, and the distribution of interfacial shear stress tends to be uniform. The bolt length can be reduced appropriately because the anchorage failure mode evolves into the tensile failure of the bolt.

Acknowledgements

The research reported in this manuscript is funded by the Natural Science Foundation of China (Grants Nos. 52179113, 42207199, 41831278). The authors wish to acknowledge Professor of CHEN Weizhong, Institute of Rock and Soil Mechanics, for his help in interpreting the significance of the results of this study.

References

- Cao GJ, Jiang HD, Xiong HM (2003) Calculation method of support length for stretched bolts. *Chin J Rock Mech Eng* 22(7): 1141-1145. (In Chinese)
<https://doi.org/10.3321/j.issn:1000-6915.2003.07.018>
- Chai J, Zhao WH, Li Y, et al (2012) Pull out tests of fiber Bragg grating sensor fitted bolts. *J China Univ Min Technol* 41(5): 719-724. (In Chinese)
<https://doi.org/10.3321/j.issn:1000-6915.2003.07.018>
- Li C, Xu JH, Li M (2013) The mechanical characteristics analysis of fully anchored prestressed bolts in coal mines. *J Mining Saf Eng* 30(2): 188-193. (In Chinese)
<http://ckxb.cumt.edu.cn/CN/Y2013/V30/I2/188>
- You CA (2005) Theory and application study on stress-transfer mechanism of anchoring system. *Chin J Rock Mech Eng* 24(7): 1272-1272. (In Chinese)
<https://doi.org/10.3321/j.issn:1000-6915.2005.07.032>
- You CA (2000) Mechanical analysis on wholly grouted anchor. *Chin J Rock Mech Eng* 19(3): 339-341. (In Chinese)
<https://doi.org/10.3321/j.issn:1000-6915.2000.03.018>
- Delhomme F, Debicki G (2009) Numerical modelling of anchor bolts under pull-out and relaxation tests. *Constr Build Mater* 24(7): 1232-1238.
<https://doi.org/10.1016/j.conbuildmat.2009.12.015>
- Farmer IW (1975) Stress distribution along a resin grouted rock anchor. *J Rock Mech Min Sci Geomech Abstr* 12(11): 347-351.
[https://doi.org/10.1016/0148-9062\(75\)90168-0](https://doi.org/10.1016/0148-9062(75)90168-0)
- Freeman TJ (1978) The behavior of fully-bonded rock bolts in the Kielder experimental tunnel. *Tunnels and Tunnelling* 10(5):37-40. [https://doi.org/10.1016/0148-9062\(78\)91073-2](https://doi.org/10.1016/0148-9062(78)91073-2)
- Wu GJ, Chu YD, Cheng WZ (2011) Constitutive model of anchorage interface in underground engineering and its time-effect analysis. *Rock Soil Mech* 32(1): 237-243. (In Chinese)
<https://doi.org/10.3969/j.issn.1000-7598.2011.01.038>
- He SM, Tian JC, Zhou JT (2006) Study on load transfer of bond prestressed anchor rope. *Chin J Rock Mech Eng* 25(1): 117-121. (In Chinese)
<https://doi.org/10.3321/j.issn:1000-6915.2006.01.019>
- Hui W, Guo YC (2016) Debonding analysis of a single anchor using catastrophe theory. *Rock Soil Mech* 37(10): 2833-2838. (In Chinese)
<https://doi.org/10.16285/j.rsm.2016.10.013>
- Li JL (2019) *Rock mechanics*, Chongqing, China. Chongqing University Press, pp 1-318 (In Chinese)
<https://www.cqup.com.cn/index.php?m=content&c=index&a=show&catid=40&id=12820>
- Li YM, Zhao CX, Li C, et al. (2019) Analysis of stress distribution characteristics of fully anchored bolt based on actual rock mass. *J China Coal Soc* 44(10): 2966-2973. (In Chinese)
<https://doi.org/10.13225/j.cnki.jccs.2018.1531>
- Wang MS, He XR, Zheng YT (1983) Mechanical model of full-length anchoring bolt and its application. *Metal mine* (04):24-29. (In Chinese)
<https://doi.org/CNKI:SUN:JSKS.O.1983-04-007>
- Lu SL, Tang L, Yang XG (1998) *Bolt anchoring force and anchoring technology*, Beijing, China. China Coal Industry Publishing Home, p 186. (In Chinese)
<https://xueshu.baidu.com/usercenter/paper/show?paperid=f382b760d001dfdf09595ed1a8ce2186>
- He SM, Zhang XG, Wang C (2004) Study on mechanism of prestressed anchoring cable based on modified shear lag model. *Chin J Rock Mech Eng* 15: 2562-2567. (In Chinese)
<https://doi.org/10.3321/j.issn:1000-6915.2004.15.016>
- Song YM, Deng LL, Lv XF, et al. (2018) Study on force transfer law of anchoring system in bolt drawing process. *Journal of mining and safety engineering* 35(06): 1122-1128. (In Chinese)
<https://doi.org/10.13545/j.cnki.jmse.2018.06.005>
- Tao Z, Chen JX (1984) Behavior of rock bolting as tunneling support. *Stephansson O ed Proceedings of the International Symposium on Rock Bolting*, Rotterdam: Balkema, pp 87-92.
<https://doi.org/10.1201/9780203740507-8>
- Esaki T, Jiang YJ, Cai Y (2003) Analytical model for grouted rock bolt design of tunnel. *Japan Society of Civil Engineers* 13: 1-6. <https://doi.org/10.1016/j.ijrmmms.2004.04.005>
- Wang XQ, Yang JH, Li JZ, et al. (2020) Mechanical characteristics analysis of full-length anchoring bolt under typical working conditions considering anchor removal. *J China Coal Soc* 45(S2): 599-608. (In Chinese)
<https://doi.org/10.13225/j.cnki.jccs.2020.0259>
- Zhu XG (2007) Study on anchoring mechanism of grouted rock bolt in underground engineering. PhD thesis, Dalian University of Technology, Dalian, China, p 153. (In Chinese)
<https://xueweilunwen.com/doc/1635866>
- Zhao YM (2012) Study on mechanical behavior of epoxy bonded bolt system and bolt bearing characteristic in coal mine roadway. *J China Coal Soc* 37(8):1423-1424. (In Chinese)
<https://doi.org/10.13225/j.cnki.jccs.2012.08.017>
- Cai Y, Esaki T, Jiang YJ (2004) An analytical model to predict axial load in grouted rock bolt for soft rock tunnelling. *Tunn Undergr Space Technol* 19(6):607-618.
<https://doi.org/10.1016/j.tust.2004.02.129>
- Zhang J, Tang B (2002) Hyperbolic function model to analyze load transfer mechanism on bolts. *Chin J Geotech Eng* 24(2): 188-192. (In Chinese)
<https://doi.org/10.3321/j.issn:1000-4548.2002.02.013>
- Jiang ZX (2001) A Gauss curve model on shear stress along anchoring section of anchoring rope of extensional force type. *Chin J Geotech Eng* 6:696-699. (In Chinese)
<https://doi.org/10.3321/j.issn:1000-4548.2001.06.010>
- Korzeniowski W, Skrzypkowski K, Herezy Ł (2015) Laboratory Method for Evaluating the Characteristics of Expansion Rock Bolts Subjected to Axial Tension / Laboratorijna Metoda Badania Charakterystyk Kotew Rozprężnych Poddanych Rozciąganiu Osiowemu. *Arch Min Sci* 60(1): 209-224.
<https://doi.org/10.1515/amsc-2015-0014>
- Korzeniowski W, Skrzypkowski K, Zagórski K (2017) Reinforcement of Underground Excavation with Expansion Shell Rock Bolt Equipped with Deformable Component. *Studia Geotechnica et Mechanica* 39(1):39-52.
<https://doi.org/10.1515/sgem-2017-0004>
- Yi YC, Zhan TB, Tan YL, et al. (2013) Research of stress distribution evolution law and influencing factors. *Journal of Mining & Safety Engineering* 30(05):712-716. (In Chinese)
<http://ckxb.cumt.edu.cn/CN/Y2013/V30/I5/712>
- Tao WB, Wu PP, Chen TL, et al. (2022) Experimental research on optimization of anchorage bearing characteristics based on bolt pull-out test. *Coal Sci Technol* 1-10. (In Chinese)
<https://doi.org/10.13199/j.cnki.cst.2020-1609>
- Li EQ, Feng JL, Xie H, et al. (2020) Numerical Analysis of Anchor Bolt Pull-out Test by Cohesive Zone Model Combined with Finite Element Method. *IOP Conf Ser: Earth Environ Sci* 570(5):052014.
<https://doi.org/10.1088/1755-1315/570/5/052014>
- Duan J, Mou C, Wang Z (2020) Experimental Investigate on Pulling out of Anchor Based on Fiber Bragg Grating Monitoring. *IOP Conf Ser: Mater Sci Eng* 741:012010.
<https://doi.org/10.1088/1757-899X/741/1/012010>
- Richard G, Christophe A, Simon R, et al. (2019) Experimental and numerical analysis of in-situ pull-out tests on rock bolts in claystones. *Eur J Environ Civ En* 25(12):2277-2300.
<https://doi.org/10.1080/19648189.2019.1626288>
- Zhao RX, Feng ZJ, Jiang G, et al. (2021) A Pull-Out Test Study on the Working State of Fully Grouted Bolts. *Fluid Dyn Mater Proc* 17(2):441-453. <https://doi.org/10.32604/fdmp.2021.010595>
- Chen J, Hagan PC, Saydam S (2016) Parametric study on the axial performance of a fully grouted cable bolt with a new pull-out test. *Int J Min Sci Technol* 26(1): 53-58.
<https://doi.org/10.1016/j.ijmst.2015.11.010>
- Forbes B, Vlachopoulos N, Diederichs MS, et al. (2020) Augmenting the in-situ rock bolt pull test with distributed optical fiber strain sensing. *Int J Rock Mech Min* 126:104202.
<https://doi.org/10.1016/j.ijrmmms.2019.104202>
- Feng Q, Jin J, Zhang S, et al. (2022) Study on a Damage Model and Uniaxial Compression Simulation Method of Frozen-Thawed Rock. *Rock Mech Rock Eng* 55:187-211.
<https://doi.org/10.1007/s00603-021-02645-2>
- Zhu ZD, Shu XY, Chen WZ, et al. (2022) Optimization study on thread connection parameters of an improved hollow grouting bolt. *J China Coal Soc* 47(06): 2300-2310.
<https://doi.org/10.13225/j.cnki.jccs.2021.1158>